International Journal of Engineering Research & Technology (IJERT)
ISSN: 2278-0181
Vol. 6 Issue 04, April-2017

Enhanced Performance of an Aramid Fiber Reinforced Polymer Reinforced (AFRP) Column with Plug and Play (PnP) Dissipater

Steve Efe (D.Eng.); Monique Head (Ph.D.)
Department of Civil Engineering,
Morgan State University, Baltimore, United States

***Abstract*-Fiber-reinforced polymer (FRP) bars gained acceptance in the construction market as a viable substitute for conventional steel bars as internal reinforcement in concrete structures. Barriers however existed in its applications where local buckling may occur relatively at low stress levels. The premature rupture and failure of FRP bars in compression members is as a result of their typically low flexural rigidity. This paper studies the response of a performance-enhanced Aramid FRP reinforced concrete column utilizing a plug-and-play connection with dissipaters to ensure elastic behavior under cyclic load and concentrating damage to the plug and play (PnP) dissipater. This paper is part of a larger numerical and experimental investigation to develop and validate design methods for a rocking AFRP reinforced concrete column. The numerical study consists of five columns, subjected to axial load followed by cyclic lateral load up to failure and analyzed using the Extreme Loading for Structures (ELS) software. Ductility and energy dissipation gains of the enhanced AFRP RC columns were compared to the conventionally reinforced column, and the influence of longitudinal bar ratio, dissipater sizes and tie spacing were investigated. Results show improve performance of the plug-and-play AFRP columns under cyclic load.**

Keywords: Aramid fiber reinforced polymer (AFRP) reinforced column; Plug-and play dissipater; Controlled rocking; Cyclic analysis; Numerical analysis.

INTRODUCTION

Bridge substructures are the most seismically susceptible during earthquake since they provide the load-resisting capacity of the bridge structural systems. Following a major earthquake, it is highly likely that bridge columns have undergone large lateral displacements necessitating replacement of the bridge structure. Research efforts have therefore been directed in recent years to the development of innovative materials, detailing and design concepts to improve bridge column damage-tolerance, post-earthquake serviceability, and to reduce eventual cost of repair. While past research have considered practical alternatives such as seismic isolation, lap splice connection, etc. to conventional seismic strengthening in minimizing potential damage, their ability to accommodate large displacement and reliability under conditions of large and repeated cyclic loading to inelastic range are of concern.

Significant effort has been dedicated in the past few years towards the development of self-centering and cost-efficient rocking connections to achieve low damage systems. [10] Recently, several construction details of unbonded post-tensioned tendons in bridge columns have been investigated to mitigate residual displacement and reduce damage caused by an earthquake. [4,9,7,16] Although these connections allow the use of modular systems, little focus has been given to the possibility of inspecting and, if necessary, replacing the tendons. Since damage is expected in the plastic hinge regions leading to substantial costs of repairing and business interruption, a controlled rocking with dissipative mechanism which allows easy mounting and replaceability of structural fuses after an earthquake event is needed to be considered before implementation. This paper examines the performance of the external rocking connection in improving the response of AFRP RC columns and limiting the longitudinal reinforcing bars strain demands.

AFRP materials due to their favorable mechanical and durability characteristics have gained permanent and growing share in the construction market with current emphasis on strengthening of RC members. Regardless, there is scarcity of relevant research outcomes and experimental evidence on their application and behavior as internal reinforcement in compression members. This is reinforced by the lack of reliable information provided by codes and specification such as ACI 440.1R-06[2] due to the brittle behavior and anisotropic nature of FRPs. To compensate for the lack of ductility in FRP bars required at the structural level in order to achieve satisfactory structural performance in compression members, the strain demands can be limited and margin of safety against FRP bars rupture can be greatly increased by allowing the member to respond elastically and ensuring stress transfer to sacrificial members.

In this paper, in order to work towards a more resilient RC column reinforced with AFRP bars that sustains little or no damage, the columns are made to respond elastically through gap opening mechanism and damage are concentrated into the PnP dissipaters. The entire column which houses the cost-efficient dissipaters have the potential to rock on its base, enabling it to survive damaging loads provided the structure does not lose its stability and overturn during the repeated cycle of loading. This PnP dissipater limits the strain demand in the AFRP reinforcing bars and also protects them from premature rupturing when the gap opens up to the design level of drift. This behavior differs from the associated damage of a conventionally reinforced column which dissipates energy

International Journal of Engineering Research & Technology (IJERT)
ISSN: 2278-0181
Vol. 6 Issue 04, April-2017

through yielding of reinforcing steel and crushing of concrete at the base of the column. The inclusion of AFRP bar as the primary longitudinal reinforcement seeks to address the deeply rooted corrosion problems in reinforced concrete (RC) bridge structures that prompt millions of dollars being spent yearly in the United States on rehabilitation projects.

LITERATURE REVIEW

A new seismic design and construction philosophy called "Damage Avoidance Design" or (DAD) was proposed to force damage to occur only in replaceable "fuses" in order to protect the structural system[7]. The investigated bridge piers were designed to rock at the top and bottom of the pier columns under lateral loading. Their finding showed that the steel armoring at the pier end zones effectively prevented premature damage to the pier.

The effectiveness of the use of post-tensioned (PT) tendon for damage-control and seismic energy dissipation has been demonstrated in precast concrete structural systems.[4,5,6,11,3] The concept is geared towards minimizing inelastic demands on the primary structure, the amount of damage needed for speedy repairs and closure time of bridges. The high-strength PT tendons are intentionally unbonded to the concrete, mostly over the column entire length, and are connected to the structures only at end anchorages. This ensures uniform distribution of tendon strains, which significantly delays yielding of the tendons, eliminates tensile stress transfer to the concrete as the strands elongate under lateral loading, thus reducing concrete cracking. As compared with conventional reinforced concrete structures, unbonded post-tensioned concrete structures offer self-centering capability and ability to undergo large non-linear lateral displacements without damage.

Numerical Analysis

The Column Models

Five (5) column specimens similar to Tobbi et al. (2012) of 13.78 x 13.78 in. (350 x 350 mm) cross-sections were considered in this numerical study to investigate the effect of longitudinal bar ratio, tie spacing, and PnP dissipater on the overall response under cyclic loading[12]. The material properties of components of the rocking columns are shown in Table 1. Specimen C1-S5N10 without the rocking connection is a steel reinforced columns having 1% longitudinal bar ratio. C2-S5N10 and C4-S5N15 are conventionally reinforced with AFRP bars (1.0% and 1.5% respectively) without the PnP dissipater. C3-S5N10 and C5-S2N10 have discontinued longitudinal FRP bars at the column-footing interface and varying PnP dissipater sizes of 5 inches and 2 inches respectively. The description of the column specimen is shown in Table 3.

The Transverse and Longitudinal Reinforcement

The AFRP bar used for the transverse and longitudinal is a technora rod made up of bundles of aramid fibres impregnated with vinylester resin. In the numerical study, it is assumed that there exist mechanical bond generated between the rod and the concrete.

The PnP dissipater

The PnP dissipater are made of mild steel bars consist of a yielding circular steel core inserted in an outer hollow steel tube to prevent the local buckling of the yielding core when in compression.. The PnP dissipater of total length of 56 inches (Figure 2) are fabricated out of 0.5 in (12.7 mm) mild steel (Grade300) plain bars while the buckling restraining tube are 1 in (25.4 mm) in diameter as shown in Table 2.

The Rocking Connection Interface

The column-footing interface has two steel plates sandwiched as shown in Figure 1. The bottom steel plate (a), which is seated on the top of the reinforcement of the footing, has a dimension of (27.6 x 27x 2 inches) 700x700x 50mm with a square hole, 510x510x64 mm at the middle to receive plate B, (20 x 20 x 2 inches) 500 x 500 x50 mm to act as a "shear key" to prevent the shoe block sliding under lateral loads. Concrete compression strength of the concrete cylinders, having152.4 mm diameter and 304.8 mm height, was measured to be $f'c$ = 4.7 ksi (32.4 N/m^2).

Table 1. Mechanical properties of concrete, AFP bars and steel.

Mechanical properties of concrete		
Parameters	Confined Concrete	
28-day compressive strength ksi (MPa)	4.7 (32.4)	
Elastic Modulus ksi (MPa)	3920 (27,028)	
Crushing Strain	17.8 E-3	
Yield Strain	2.3E-3	
Mechanical properties of AFRP (Technora rod) reinforcement		
Tensile Strength ksi (MPa)	203 (1400)	
Elastic Modulus ksi (MPa)	10000 (68950)	
Ultimate Tensile Strain	0.0203	
Ultimate Compressive Strain	7.2E-3	
Mechanical properties of steel		
Steel Material and Grade	A615 Grade 60	A615 Grade 40
Yield Stress ksi (MPa)	60 (413.68)	40 (275.79)
Fracture Stress, ksi (MPa)	90 (620.52)	70 (482.63)
Failure Strain	0.15	0.14
Elastic Modulus ksi (GPa)	29E+3 (200)	29E+3 (200)

International Journal of Engineering Research & Technology (IJERT)
ISSN: 2278-0181
Vol. 6 Issue 04, April-2017

Table 2. PnP disspater details

PnP dissipater details	
Parameters	Confined Concrete
Dissipater size in. (mm)	0.5 (12.7)
Buckling restraining tube size in. (mm)	1 (25.4)
Yielding Stress ksi (MPa)	270 (1860)
Initial Stress ksi (MPa)	90 (620.5)
Grade of Steel	Mild Steel

Modeling

The modeling and analysis was carried out in the 3-D environment of Extreme Loading Software (©ELS), an advanced structural analysis software package that uses Applied Element Method (AEM) to track structural collapse behavior. The program is capable of predicting the large displacement behavior of 2D and 3D structures under static and dynamic loads, taking into account geometric nonlinearities and the effect of material inelasticity. To a high degree of accuracy, ELS enables proper understanding of the materials behavior from elastic to plastic stages including cracking, large displacements, reinforcement yielding, complete element separation and collapse. ELS has pre-defined styles with linear and nonlinear materials models which could be modified to suit the composition of the controlled rocking column system. Each section of the columns consists of a number of concrete and reinforcement fibers, as shown in Figure 1. The concrete fibers represent the confined (core) concrete ($n_c = 460$ fibers) and the unconfined cover concrete ($n_{uc} = 296$ fibers) of the column. The steel or AFRP fibers represent the longitudinal reinforcement. The confined, core concrete has a higher maximum compressive strength and reduces to a lower strength as the strain increases, representative of the strength of the confined core after the cover has spalled off. The unconfined cover concrete decreases to zero stress once the cover cracks and spalls because it can no longer carry any load. The 8-node regular hexahedron elements were used to model the column, load cap and foundation, while the reinforcement bars and stirrups were adequately captured using the software's modified custom reinforcement, and the energy dissipaters using ELS link element housed in a duct and spans between two end plates as shown in Figure 1.

Table 3. Column Description

Specimen ID	Long. Bar Type	Long Bar Continuity	Tie Bar Type	Percentage Long. Reinf. Bar (%)	Tie spacing (mm)
C1-S5N10	Steel	YES	Steel	1.0	127
C2-S5N10	AFRP	YES	AFRP	1.0	127
C3-S5N10	AFRP	NO	FRP	1.0	127
C4-S5N15	AFRP	YES	FRP	1.5	127
C5-S2N10	AFRP	NO	FRP	1.0	50.8

Table 4: Parametric Study

No.	Specimens	Parameters studied
1	C1-S5N10	Steel columns without dissipater
2	C4-S5N15	AFRP Column with 2% Percentage of longitudinal bar
3	C5-S2N10	AFRP RC with dissipater with reduced tie spacing
4	C2-S5N10	AFRP RC without dissipater
5	C3-S5N10	AFRP RC reinforced columns with dissipater

Due to the anticipated stress concentration and crack spacing at the plastic hinge zone, a smaller mesh-size (halved) compared to other areas was used for the shoe block. Translational degrees of freedom in the x, y and z global axes directions of the elements in contact with the ground were fixed, hence creating the necessary support condition at the base. Also, to capture the behavior of the concrete before and after cracking, the compression model (Figure 3a and b) is adopted[13] while the model presented in Figure 3c is used for the reinforcement[14].

For the AFRP material, a linear elastic model up to failure stress is used (Figure 3). Since the program is capable of automatically determining the location of plastic hinges during loading, trial and error assumptions about which areas are prone to failure are eliminated. In the analysis, material strain from elastic to plastic deformation provided the criteria for adjudging damage concentration and failure of the controlled rocking columns system while drift performance serves as means of comparison.

International Journal of Engineering Research & Technology (IJERT)
ISSN: 2278-0181
Vol. 6 Issue 04, April-2017

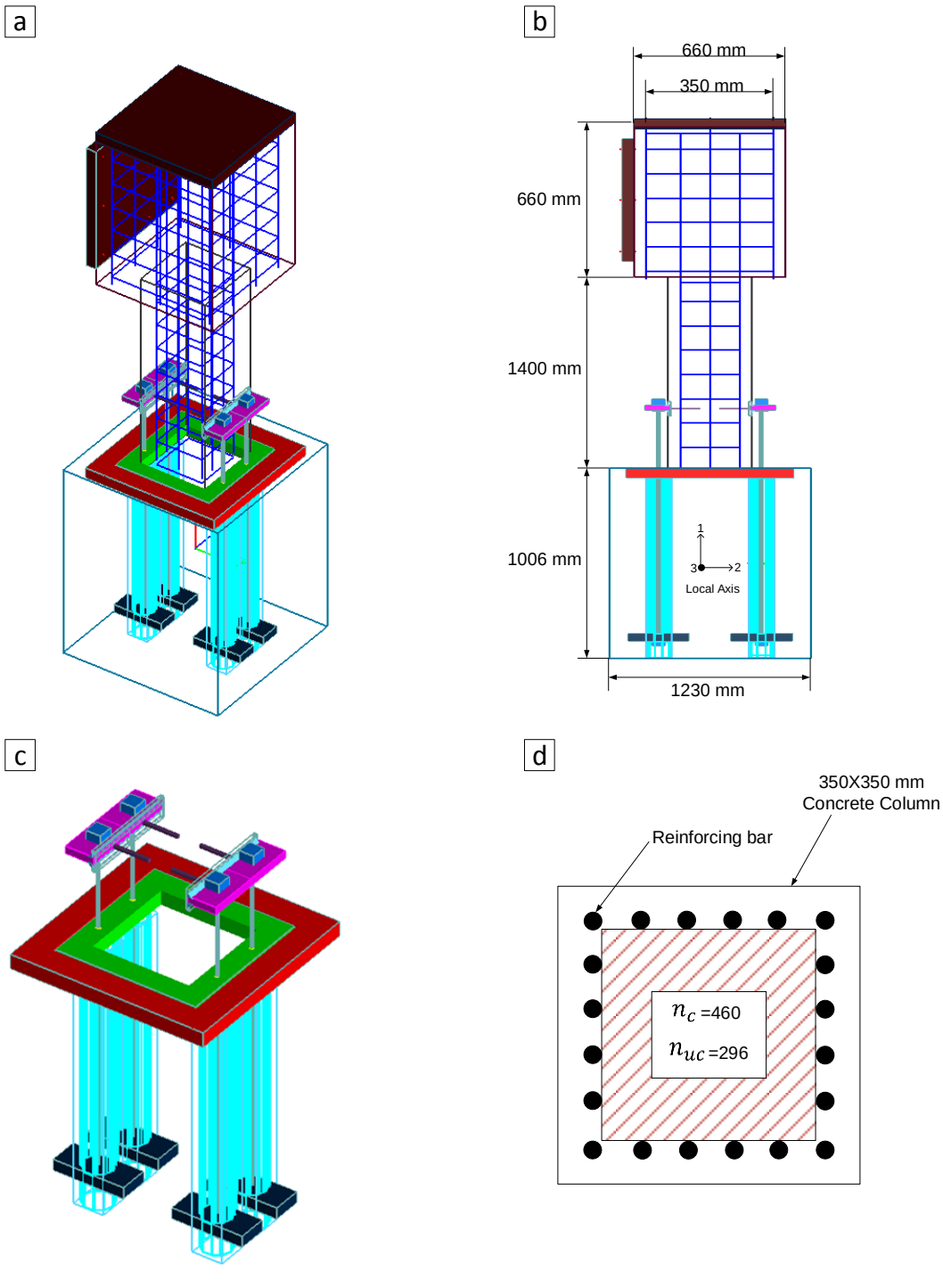

Figure 1. Column showing the 3D model of the specimen and rocking connection, (a) Model perspective view, (b) Model section view and local axis, (c) 3D rocking connection, (d) Column cross section

International Journal of Engineering Research & Technology (IJERT)
ISSN: 2278-0181
Vol. 6 Issue 04, April-2017

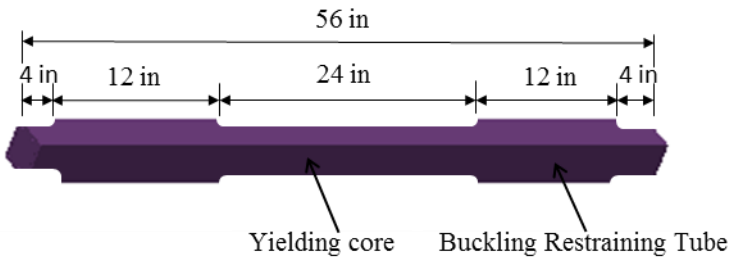

Figure 2. ELS Model of the PnP Dissipater

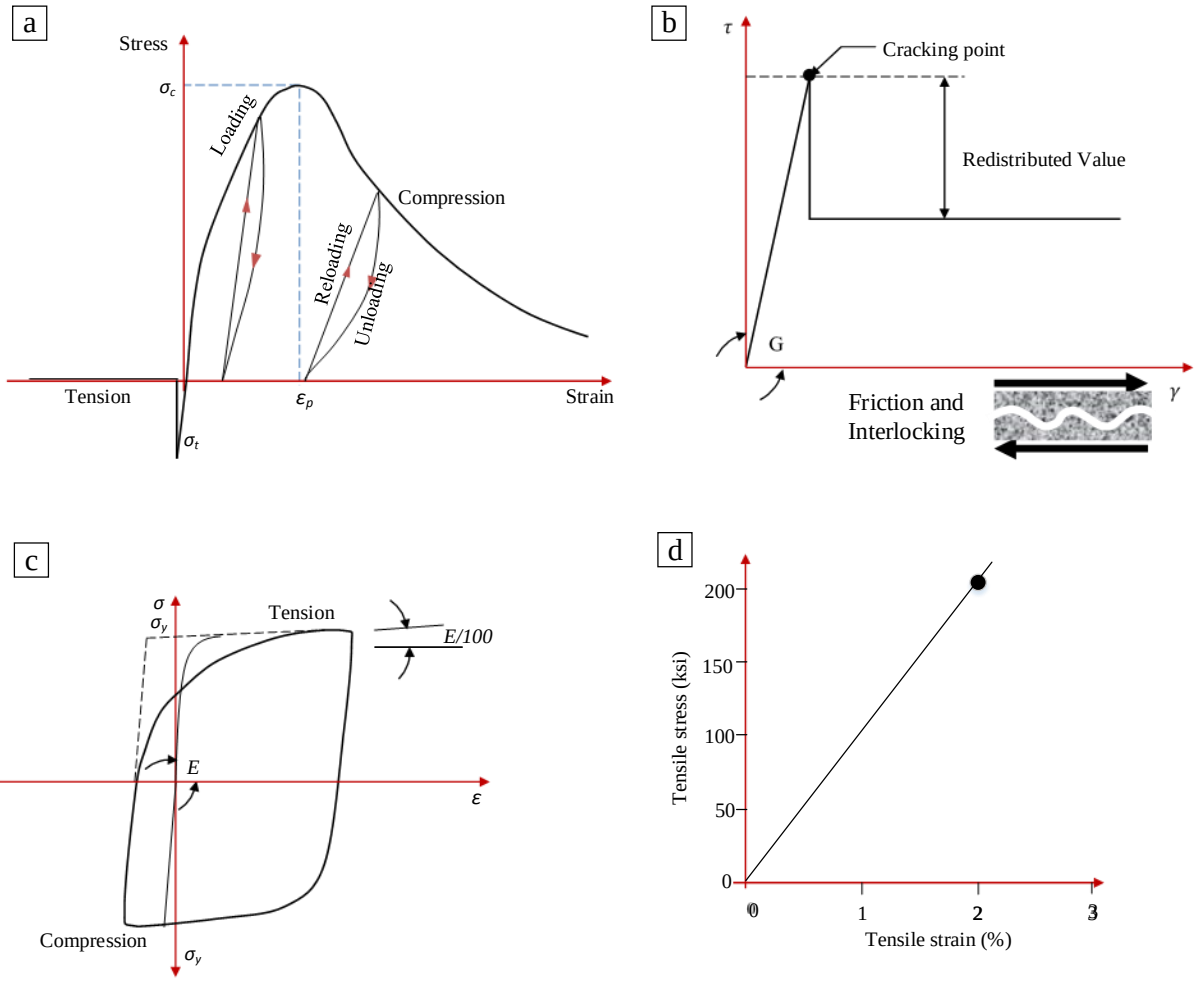

Figure 3. Constitutive models for concrete, steel and AFRP bars, (a) Concrete under axial stress [12], (b) Concrete under shear stresses [12],(c) Constitutive models for steel reinforcement[14], (d) Tensile stress-strain characteristics of AFRP [15].

Failure Criteria

The reinforcement failure criterion is satisfied by having a normal stress equal or greater than the ultimate stress specified for the reinforcement bar stress (Tagel-Din, 2009). In all the AFRP columns, the bars whose material follows a linear elastic behavior up to tension failure, are specified to be in tension since bar rupture in ELS only works with bars in tension. Also, the mild steel bars i.e. energy dissipaters are expected to fail if its stress reaches the ultimate stress or if the concrete reaches the separation strain of 0.15 (Tagel-Din, 2009).

The Controlled Rocking System and Expected Behavior

The rocking AFRP RC columns consist of a footing, a square column (350x350x1550mm) with the head block forming the primary modular elements of the system while the rocking connection representing the secondary element, consists of the unbonded dissipater made of mild steel bar which sits externally to the column and is housed in a duct in the foundation (Figure 4). To achieve the primary objective of the rocking connection, this study considers the stability of the column under axial load and bending as well as possibility of failure of the columns cross section above the column-foundation interface. A mild steel energy dissipater spans between the

International Journal of Engineering Research & Technology (IJERT)
ISSN: 2278-0181
Vol. 6 Issue 04, April-2017

two ends of the ASTM A572 Grade 50 steel plate having round holes 1/16 in. larger than the bolt diameter and firmly held using bolts. The steel plates are in turn welded to plates firmly located in the column ensuring adequate shear transfer by friction. Fillet welds of 1-in. thick are obtained based on weld design which was less than minimum weld size of 1-3/4 in. stated in Section 2.4.5 of the Structural Welding Code.[1] The minimum weld size of 1-3/4 in. was therefore considered in this study. Lesser thickness of weld could rupture which would have detrimental effect on the stability performance of the dissipater and the overall system.

The columns which are expected to reach large displacement demands would have the longitudinal AFRP bars undergo low strain demands and prevent them from possibility of rupture. When loaded laterally, a gap at the column to foundation interface will open and stretch the dissipater, which would generate a rocking force at the top of the connection (Figure 5). Shear capacity is provided by the column and its base plate that goes inside the foundation (those angles), and moment capacity of the connection by dissipaters. In order to safely transfer this rocking force through the connection and into column, steel armor plates are cast in the column and foundation respectively. Also, ducts are provided to house energy dissipater inside the foundation to ease installation and replacement.

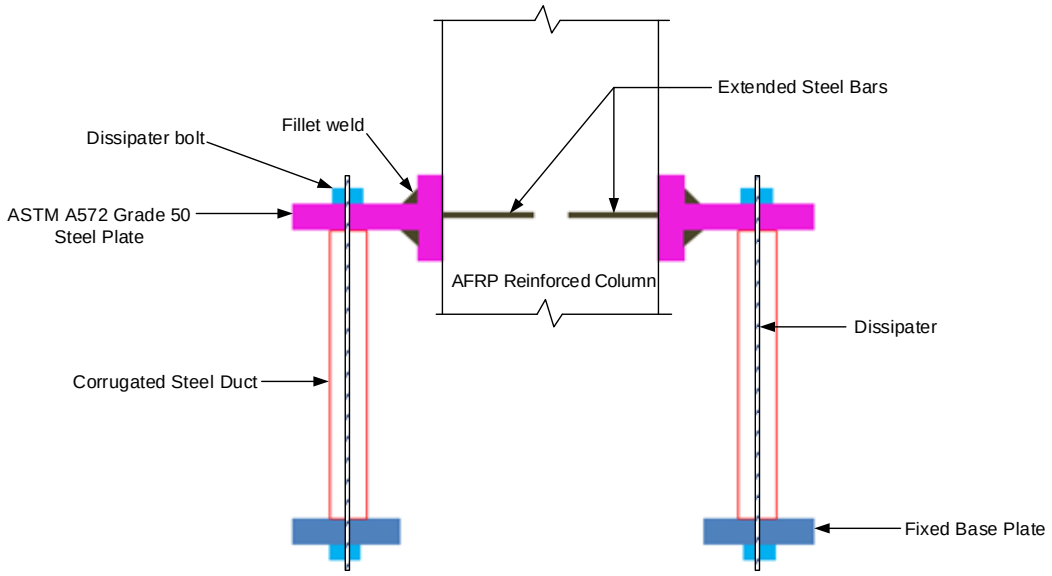

Figure 4. Rocking connection with PnP dissipater

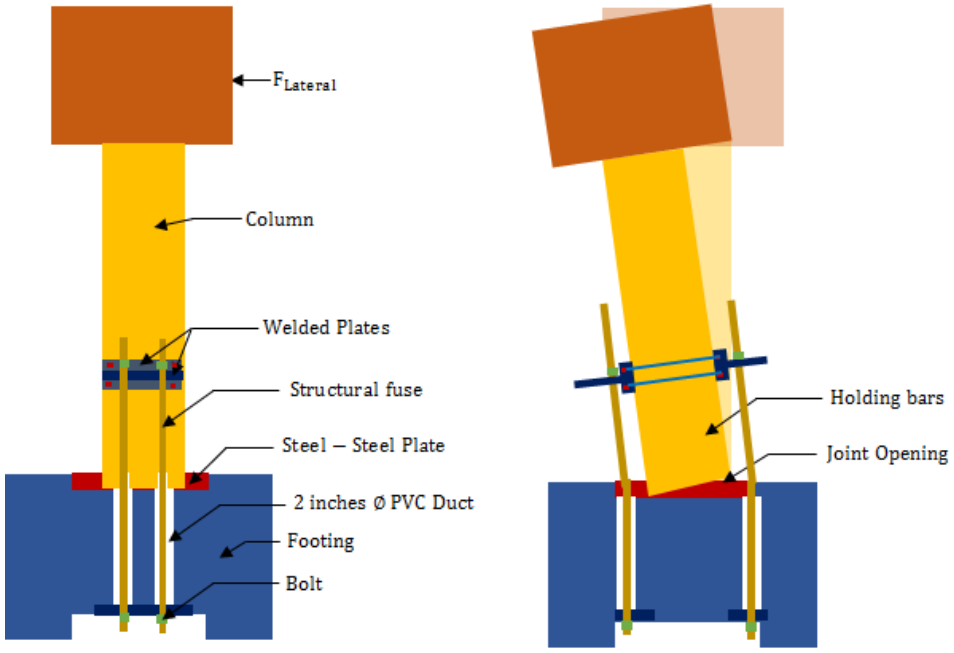

Figure 5. Rocking behavior of the column (a) Column and rocking components (b) Column Response under loading (view rotated 90 degrees).

International Journal of Engineering Research & Technology (IJERT)
ISSN: 2278-0181
Vol. 6 Issue 04, April-2017

3.1 Loading

A reverse cyclic lateral load analysis was performed to evaluate the performance of the columns with the cycles of each analysis conducted in displacement control (Figure 6).

The column lateral force-displacement responses for specimens are shown in Figures 8 to 10. The column drift is defined as the displacement at the level of the applied load divided by the column height to the applied load.

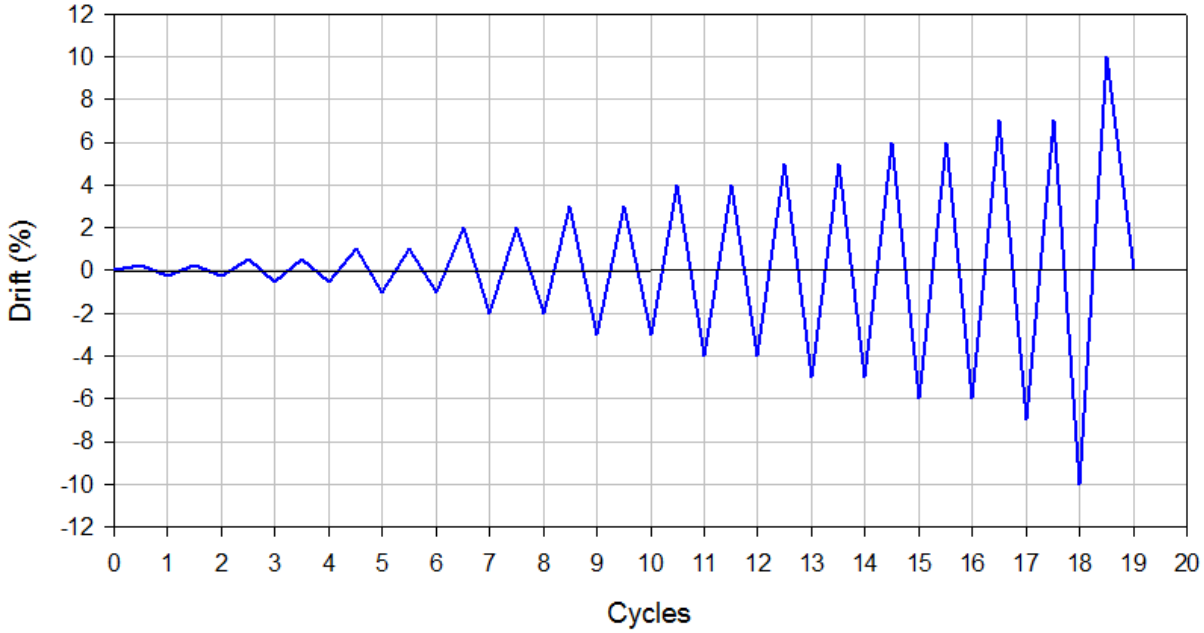

Figure 6. Load Cycle for Analytical Study

3.2 Ductility and Energy Dissipation

The ductility performance of each column was examined according to ductility and energy-based indicators in order to assess the inelastic performance and energy dissipation capacity of the columns. The average envelope curve [8] was estimated from the cyclic response of each specimen as shown in Figure 7a where it can show that.

$$\Delta_i = \left(\frac{\Delta_{i^-} + \Delta_{i^+}}{2}\right) \quad (1)$$

$$H_{imax} = \left(\frac{H_{i^-} + H_{i^+}}{2}\right) \quad (2)$$

$$K_i = \left(\frac{K_{i^-} + K_{i^+}}{2}\right) \quad (3)$$

A bilinear diagram in Figure 7b is derived from the load-displacement envelope by Park (1989) as shown in Figure 7. The maximum horizontal load carried by the column after the yielding is given as H'_{max}. This represents the beginning of the post-peak behavior of the columns. The bilinear curve consist of a straight line from the origin which passes through the envelope curve at a load of $0.75H'_{max}$ or at the yielding load (whichever is less), and it is then extended until the intersection with H'_{max}. From the newly established point (Δ_{yl}, H'_{max}), a straight line is extended to a second point (Δ_2, H'_2), where Δ_2 is the failure displacement and H'_2 is the horizontal load equal to 80% of H'_{max}.

The idealized structural ductility [8] is defined as

$$\mu_{\Delta l} = \frac{\Delta_2}{\Delta_{yl}} \quad (4)$$

The energy dissipated during one cycle i, E_i, is described by the hatched area in Figure 6b. The total dissipated energy during the test E_{hyst}, until 80% of conventional failure or bar rupture is reached [8] is defined as:

$$E_{hyst} = \frac{1}{H'_{max}\Delta_{yl}} \sum_{i=1}^{n} E_i \quad (5)$$

where the energy E_i [8] can simply be computed as:

$$E_i = \frac{(H'_{max})_i(\Delta_{max})_i}{2} \quad (6)$$

where H'_{max} is the maximum equivalent lateral load, which includes the applied horizontal load, and the equivalent horizontal load due to the P-Δ effect, if applicable.

A damage index DEW, which combines the cyclic dissipated energy and the elastic energy [8] is defined as:

$$D_{EW} = \frac{1}{H'_{max}\Delta_{yl}} \sum_{i=1}^{n} E_i \left(\frac{K_i}{K_{yl}}\right)\left(\frac{\Delta_i}{\Delta_{yl}}\right)^2 \quad (7)$$

where K_i and Δ_i are defined in Figure 7 a.

International Journal of Engineering Research & Technology (IJERT)
ISSN: 2278-0181
Vol. 6 Issue 04, April-2017

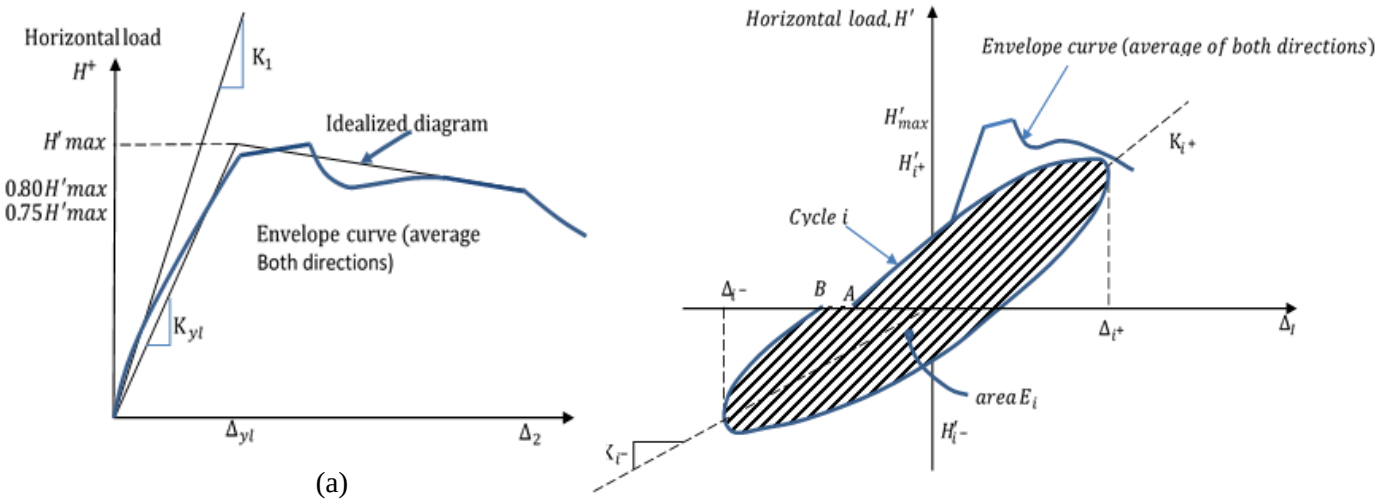

Figure 7. Energy dissipation curve [21], (a) Ideal curve definitions, (b) Hysteresis curve and energy dissipation.

Analytical Results

a) Influence of dissipater on AFRP RC Column (C1-S5N10 vs. C3-S10N10).

The presence of the PnP dissipater has an important influence on the overall behavior of the columns. Figure 8a and 8b show the cyclic lateral load-displacement of columns C1-S5N10 and C3-S10N10 predicted by ELS. The residual displacement of column C3-S10N10 is negligible compared to the conventional steel RC column C1-S5N10 due to the restoration capability of the PnP dissipater which returns the column to its intact position in the unloading stages. Columns C1-S5N10 with longitudinal steel bars continuous into the footing experienced large amount of cracks, early failure and induced damage during loading and unloading. Failure of C3-S10N10 occurred immediately after the strain in the dissipater reached its failure strain ($\varepsilon_t = 0.002$). Column C3-S10N10 has an ultimate load of 22.4 kips at 5.6% drift. C1-S5N10 failed at a lower displacement level and damage index, D_{EW} is 20.2 which is lower than column C3-S10N10 damage index of 16.7. C1-S5N10 total energy dissipated is 57% lower than C4-S5N10 (Table 8). The failure of C1-S5N10 occurred as a result of the damage to the steel rebars and concrete fibers at the plastic region. Column C3-S10N10 failure occurred due after the fracture of PnP dissipaters with no damage to the AFRP bars.

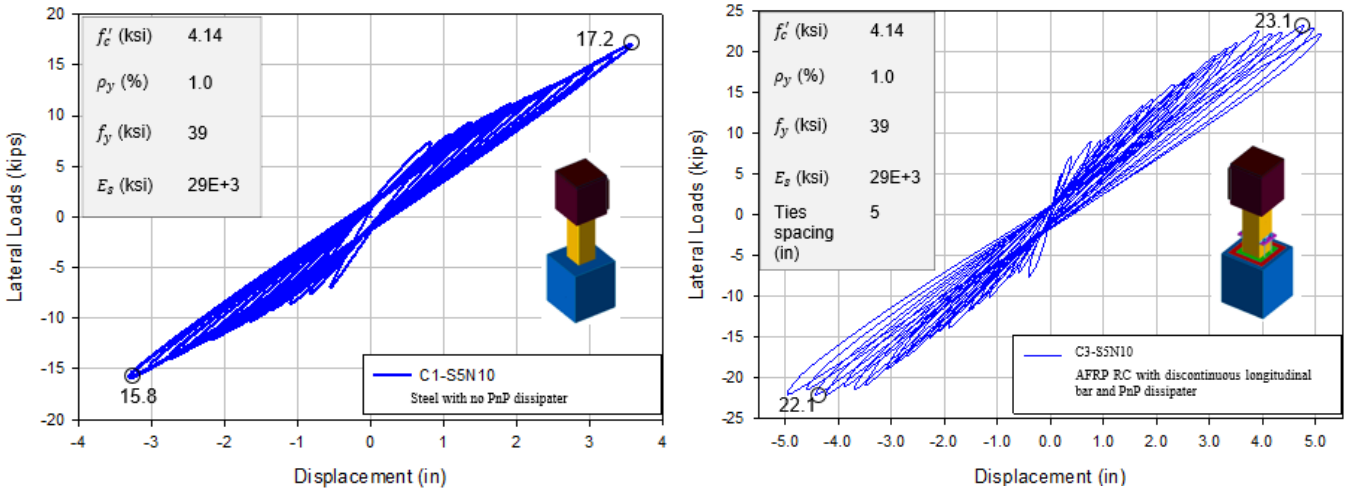

.(a) (b)

Figure 8: Effect of dissipater presence on Steel and AFRP RC Columns, C1-S5N10 and C3-S10N10

c)Effect of percentage of longitudinal bar on AFRP RC column with dissipater (C2-S5N10 and C4-S5N10)

Figures 9a and 9b show the cyclic lateral load-displacement of columns C2-S5N10 and C4-S5N10 predicted by ELS. Failure in the two columns occurred as a result of rupture of the dissipaters. A lateral load capacity difference of less than 5% is observed for the two columns. This means increase in the percentage of longitudinal bars do not significantly improve the lateral performance of the rocking columns. C2-S5N10 damage index, D_{EW} is 17

International Journal of Engineering Research & Technology (IJERT)
ISSN: 2278-0181
Vol. 6 Issue 04, April-2017

which is 14% and 17% lesser than C4-S5N10, while the hysteresis energy dissipated was higher for column C2-S5N10 (Table 5).This means an increase in the AFRP bar percentage does not necessarily increase the energy dissipation capacity of the columns since the dissipater provides the rocking mechanism and prevents the AFRP bars from being load bearing.

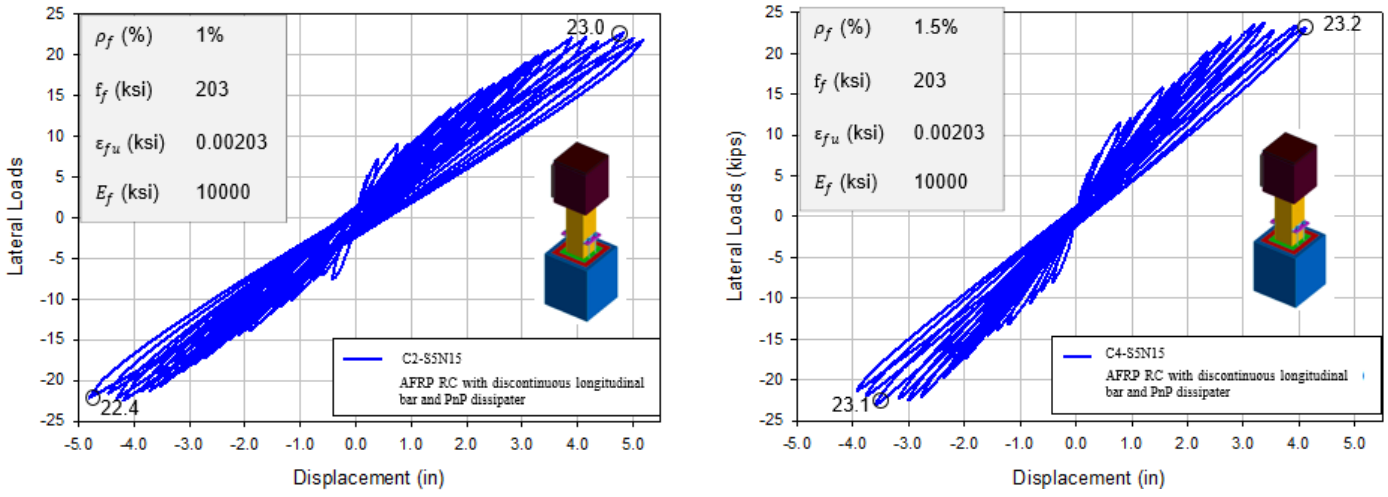

.(a) (b)

Figure 9: Influence of percentage of longitudinal bar on AFRP RC Columns C2-S5N10 and C4-S5N10

d) Influence of tie spacing on the AFRP RC columns (C3-S10N10 and C5-S2N10) with the PnP dissipater

Figures 10a and 10b show the load-displacement hysteretic performance of the two columns. Column C5-S2N10 and C3-S10N10 which had a tie spacing of 2 inches and 5inches respectively has a lateral load capacity difference of 3%. However, increase in the tie spacing resulted in significant decrease in the lateral load performance of the column by 7%. C5-S2N10 damage index, D_{EW} is 15 which is 3% lesser than the indexes of columns C3-S5N10, while the hysteresis energy dissipated higher in C3-S5N10 (Table 5). Decreasing the tie spacing gives better confinement thus improved the damage performance of the FRP columns but has little or no effect on the drift performance of the columns.

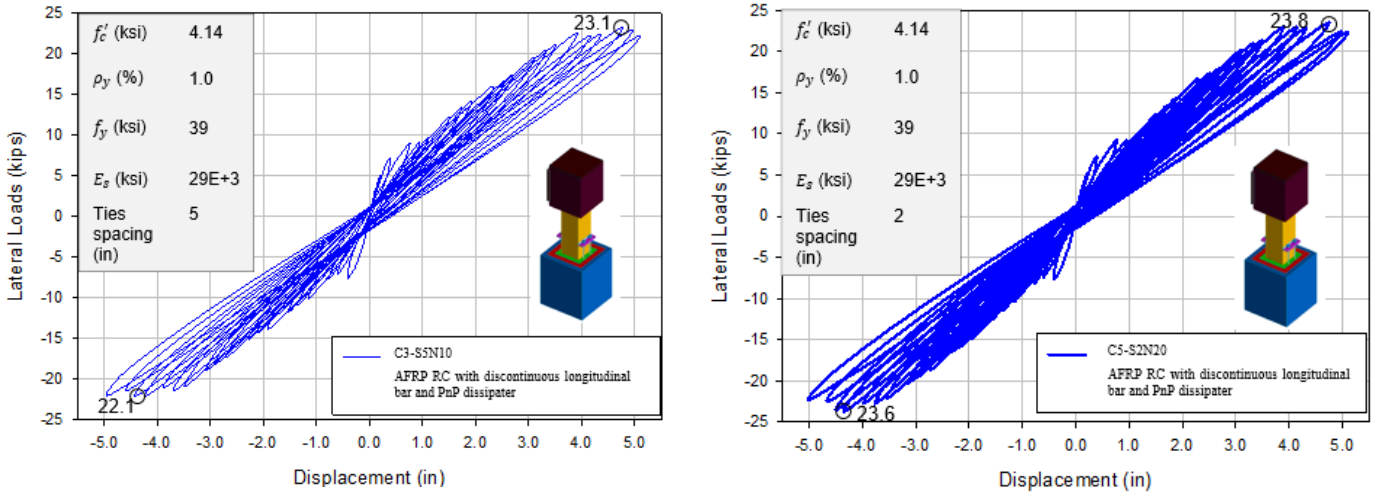

.(a) (b)

Figure 9: Effect of tie spacing on the AFRP RC columns C3-S10N10 and C5-S2N10

Damage progression (C1-S5N10 vs. C5-S2N10)

The behavior of the conventional Steel RC and rocking AFRP RC columns differs significantly from the onset to point of collapse or failure (Figures 13). At about 1.2 percent drift ratio, the longitudinal steel in column C1-S5N10 yielded and the first significant horizontal cracks appeared (Figure 9). Increase in loading at 1.8% drift resulted in fracture of the longitudinal steel and concentration of damage in the plastic hinge region. However, during uplift, column C5-S2N10 had no or

International Journal of Engineering Research & Technology (IJERT)
ISSN: 2278-0181
Vol. 6 Issue 04, April-2017

insignificant cracks developed along the column height and the longitudinal AFRP bars experienced insignificant strain ($\varepsilon_{t,max} < 0.0004$). Notwithstanding the collapse of the AFRP rocking column C5-S2N10 at 5.6% drift was due to the failure of the dissipater, while the longitudinal AFRP bars in the column did not reach their yield strain ($\varepsilon_t \ll 0.001$).

Table 5. Energy and Damage Assessment

Specimen ID	Column drift (%)	H_{max} (kip)	Δ_{yl} (in)	Δ_2 (in)	$\mu_{\Delta l}$	E_{hyst}	K_i (kips/in)	K_{yl} (kips/in)	D_{EW}
C1-S5N10	4.0	17.0	1.2	3.6	3.0	22.8	15.2	14.2	20.2
C2-S5N10	5.7	22.6	1.7	5.2	3.1	35.8	15.6	13.3	17.2
C3-S10N10	5.6	23.8	2.0	5.1	2.6	32.9	12.6	12.0	16.7
C4-S5N15	4.6	23.2	1.5	4.2	2.8	33.6	16.1	15.5	19.7
C5-S2N10	5.6	23.7	2.3	5.1	2.2	37.8	12.0	10.2	15.3

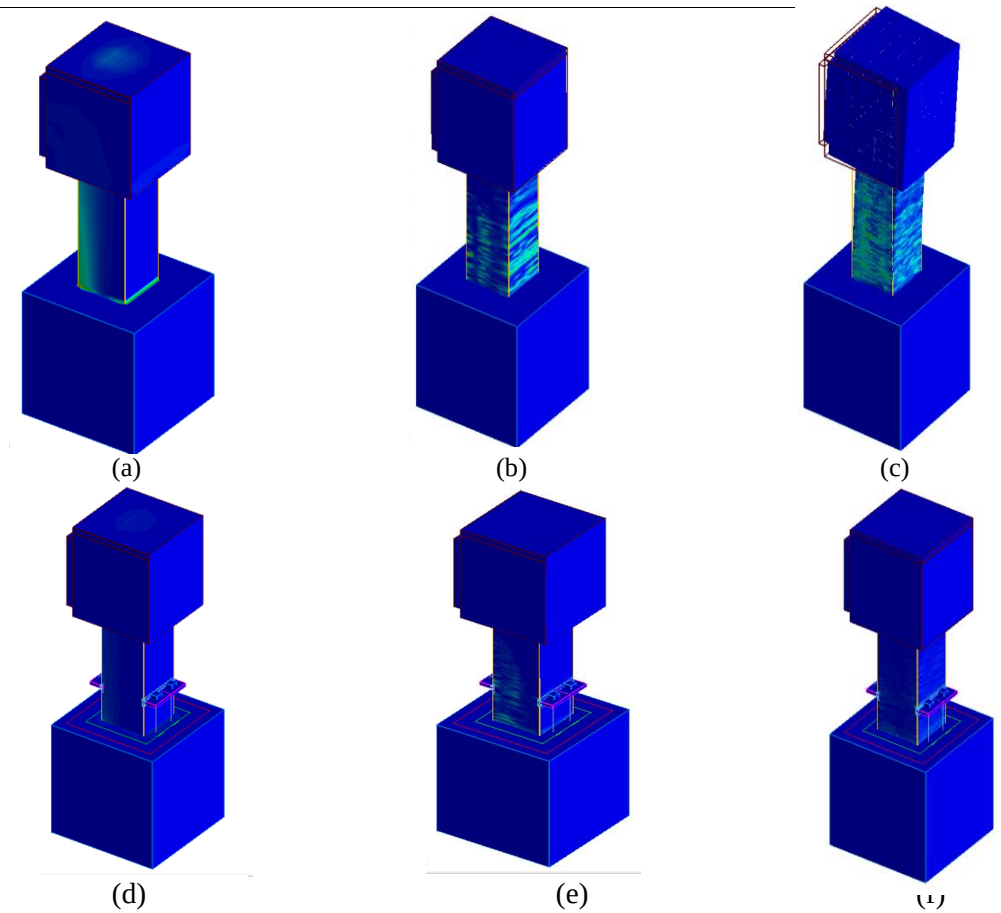

Figure 9. Damage progression of column showing strain profile, (a) Significant concrete crack at 1% drift for conventional column C1-S5N10, (b) Concrete crushing at 2.2% drift for conventional column C1-S5N10, (c) Failure at 2.5 drift for conventional column C1-S5N10, (d) First crack at column-footing interface at 0.3 % drift for rocking column C5-S2N10, (e) Column at 2.2% drift for rocking column C5-S2N10, (f) Column failure at 4.5% drift is due to dissipater fracture in rocking column C5-S2N10.

4 CONCLUSIONS

The numerical results presented in this paper shows the possibility of improving the performance of AFRP RC column and mitigating damage to the internal reinforcing bars through the provision of externally mounted dissipater. The following conclusion can be made based on response prediction by ELS.

1. Concentrated damage at the plastic region experienced in conventional columns during loading was overcome as these were transferred to secondary elements (dissipater) which provided re-centering capabilities. Failure in the rocking columns occurred once the dissipater reaches its failure strain.

2. The rocking AFRP columns experienced better energy dissipation and lower damage index than the conventional column. A further refinement of the model with a secondary element to prevent sudden collapse of the AFRP RC columns after failure of the dissipater is needed.

3. dissipater rocking connections performed as expected. However, for practical use of the proposed connection and optimized effectiveness of response, investigation to find appropriate dissipater size and height above the column-footing interface to suit performance requirement is essential.

International Journal of Engineering Research & Technology (IJERT)
ISSN: 2278-0181
Vol. 6 Issue 04, April-2017

REFERENCES

[1] AWS, D. (2006). D1. 1/D1. 1M-Structural Welding Code-Steel. American Welding Society.

[2] ACI Committee 440. (2007). Guide for the Design and Construction of Structural Concrete Reinforced with FRP Bars. American Concrete Institute.

[3] Burningham, C. A., Pantelides, C. P., & Reaveley, L. D. (2015). Repair of reinforced concrete deep beams using post-tensioned CFRP rods.Composite Structures, 125, 256-265.

[4] Hewes, J. T., & Priestley, M. N. (2002). Seismic design and performance of precast concrete segmental bridge columns (No. SSRP-2001/25).

[5] Kurama, Y., Pessiki, S., Sause, R., & Lu, L. W. (1999). Seismic behavior and design of unbonded post-tensioned precast concrete walls. PCI journal,44(3), 72-89.

[6] Kurama, Y. C., & Shen, Q. (2004). Posttensioned hybrid coupled walls under lateral loads. Journal of Structural Engineering, 130(2), 297-309.

[7] Mander, J. B., & Cheng, C. T. (1997). Seismic resistance of bridge piers based on damage avoidance design. In Technical Report NCEER (Vol. 97). US National Center for Earthquake Engineering Research (NCEER).

[8] Osorio, L. I., Paultre, P., Eid, R., & Proulx, J. (2014). Seismic behavior of synthetic fiber-reinforced circular columns. ACI Structural Journal, 111(1), 189.

[9] Ou, Y. C., Wang, P. H., Tsai, M. S., Chang, K. C., & Lee, G. C. (2009). Large-scale experimental study of precast segmental unbonded posttensioned concrete bridge columns for seismic regions. Journal of structural engineering, 136(3), 255-264.

[10] Palermo, A., Pampanin, S., & Marriott, D. (2007). Design, modeling, and experimental response of seismic resistant bridge piers with posttensioned dissipating connections. Journal of Structural Engineering, 133(11), 1648-1661.

[11] Perez, F. J., Pessiki, S., & Sause, R. (2004). Seismic design of unbonded post-tensioned precast concrete walls with vertical joint connectors. PCI journal, 49(1), 58-79.

[12] Qureshi, K. M. J. Stress Transfer across Interfaces in Reinforced Concrete due to Aggregate Interlock and Dowel Action.

[13] Ristic, D., Yamada, Y., & Iemura, H. (1986). Stress-strain based modeling of hysteretic structures under earthquake induced bending and varying axial loads. Research Rep. No. 86-ST, 1.

[14] Tagel-Din, H. (2009). High fidelity modeling of building collapse with realistic visualization of resulting damage and debris using the applied element method. Rep. No. HDTRA1-09-P-0006, Defense Threat Reduction Agency (DTRA), Washington, DC.

[15] Tobbi, H., Farghaly, A. S., & Benmokrane, B. (2012). Concrete columns reinforced longitudinally and transversally with glass fiber-reinforced polymer bars. ACI Structural Journal, 109(4), 551.

[16] Yamashita, R. (2005). Shake Table Testing and an Analytical Study of an Unbonded Prestressed Hollow Concrete Columns Constructed with Precast Segments (Doctoral dissertation, University of Nevada, Reno).